

# Genome-wide transcriptional analysis of the human cell cycle identifies genes differentially regulated in normal and cancer cells

Ziv Bar-Joseph<sup>\*†‡</sup>, Zahava Siegfried<sup>§</sup>, Michael Brandeis<sup>¶</sup>, Benedikt Brors<sup>||</sup>, Yong Lu<sup>\*</sup>, Roland Eils<sup>||\*\*</sup>, Brian D. Dynlacht<sup>††</sup>, and Itamar Simon<sup>§‡</sup>

<sup>\*</sup>Department of Computer Science, School of Computer Science and <sup>†</sup>Lane Center for Computational Biology, Carnegie Mellon University, Pittsburgh, PA 15213;

<sup>§</sup>Department of Molecular Biology, Hebrew University Medical School, Jerusalem 91120, Israel; <sup>¶</sup>Department of Genetics, Alexander Silberman Institute of Life Sciences, Hebrew University, Jerusalem 91904, Israel; <sup>||</sup>Department of Theoretical Bioinformatics, German Cancer Research Center, Im Neuenheimer Feld 580, D-69120 Heidelberg, Germany; <sup>\*\*</sup>Department of Bioinformatics and Functional Genomics, Institute of Pharmacy and Molecular Biotechnology, University of Heidelberg, D-69115 Heidelberg, Germany; and <sup>††</sup>Department of Pathology and New York University Cancer Institute, New York University School of Medicine, New York, NY 10016

Edited by Clare McGowan, The Scripps Research Institute, La Jolla, CA, and accepted by the Editorial Board December 4, 2007 (received for review May 20, 2007)

**Characterization of the transcriptional regulatory network of the normal cell cycle is essential for understanding the perturbations that lead to cancer. However, the complete set of cycling genes in primary cells has not yet been identified. Here, we report the results of genome-wide expression profiling experiments on synchronized primary human foreskin fibroblasts across the cell cycle. Using a combined experimental and computational approach to deconvolve measured expression values into “single-cell” expression profiles, we were able to overcome the limitations inherent in synchronizing nontransformed mammalian cells. This allowed us to identify 480 periodically expressed genes in primary human foreskin fibroblasts. Analysis of the reconstructed primary cell profiles and comparison with published expression datasets from synchronized transformed cells reveals a large number of genes that cycle exclusively in primary cells. This conclusion was supported by both bioinformatic analysis and experiments performed on other cell types. We suggest that this approach will help pinpoint genetic elements contributing to normal cell growth and cellular transformation.**

deconvolution | expression profile

**T**ight regulation of the cell cycle is necessary for the proper growth and development of all organisms. Dysregulation of cell cycle controls leads to proliferative diseases, most notably cancer. One approach to understanding basic cell cycle processes and their deregulation in cancer has been genome-wide characterization of the cell cycle transcriptional program (1). In these microarray experiments, the RNA levels of every gene is measured in a synchronized cell population at multiple time points. Synchronization is achieved by releasing cells from a cell cycle arrest. This approach was carried out initially to characterize the yeast cell cycle, and, subsequently, it was applied to examine the cell cycle in multiple organisms (reviewed in ref. 2).

Although arrest methods were effective for characterizing cycling genes in a number of species (3–7), they did not lead to complete synchronization, even for yeast cells (8–10). A number of methods were introduced for resynchronizing yeast cells by either matching the profiles for the first and second cycle for each gene (9) or by combining expression and bud count information to reconstruct the expression profile (8). These methods were shown to improve (the already good) yeast cell cycle expression data. However, these methods cannot be directly applied to mammalian cells because of two major differences between yeast and mammalian cells: (i) normal diploid mammalian cells lose their synchronization relatively soon after release of growth arrest (11) and (ii) only 50–70% of wild-type mammalian cells reenter the cell cycle after release from arrest (12). The large percentage of arrested cells and loss of synchro-

nization means that expression values represent a mixed population of cells, which introduces high background noise that confounds differentiation between genuine cell cycle-regulated genes and randomly fluctuating genes. This may have contributed to the problem encountered in a study that used synchronized human fibroblasts for the identification of cycling genes (13, 14).

So far, there have been few attempts to tackle this problem. CheckSum (15), a quality control method for time series expression data, can detect cases in which genes are missed because of synchronization loss. However, CheckSum cannot reconstruct the profiles of the missed genes, and so it cannot recover the cyclic expression patterns in primary cells. A different approach to overcome these difficulties was introduced by Whitfield *et al.* (16), who used a transformed cell line (HeLa), which is easier to synchronize, to identify cycling genes. However, these cells may not display the normal pattern of gene expression seen in nontransformed human cell types but rather reflect the proliferative nature of transformed cells in culture.

In light of these limitations, we do not have a complete gene expression dataset of the normal human cell cycle. To overcome this problem, we developed a combined experimental and computational approach that addresses the limitations of mammalian cell cycle experiments and leads to the identification of true cell cycle expression profiles from “noisy” data. Our approach uses information about the degree of synchronization of the culture and the percentage of cells reentering the cell cycle (obtained empirically by FACS analysis) to deconvolve the expression profiles of genes. Cycling genes are identified by using these corrected profiles. We reconstructed cell cycle profiles by carrying out new microarray experiments, using (partially) synchronized primary human foreskin fibroblasts. Analysis of the reconstructed profiles and comparison with published expression datasets from transformed cells reveals a large number of genes that cycle in primary cells and not in transformed cells.

Author contributions: Z.B.-J. and Z.S. contributed equally to this work; Z.B.-J., B.D.D., and I.S. designed research; Z.S. and M.B. performed research; Z.B.-J. contributed new reagents/analytic tools; Z.B.-J., B.B., Y.L., R.E., and I.S. analyzed data; and Z.B.-J., Z.S., B.D.D., and I.S. wrote the paper.

The authors declare no conflict of interest.

This article is a PNAS Direct Submission. C.M. is a guest editor invited by the Editorial Board.

Data deposition: Expression profiles have been deposited in the European Bioinformatics Institute ArrayExpress database, [www.ebi.ac.uk/arrayexpress](http://www.ebi.ac.uk/arrayexpress) (accession no. E-TABM-263).

<sup>†</sup>To whom correspondence may be addressed. E-mail: [zivbj@cs.cmu.edu](mailto:zivbj@cs.cmu.edu) or [itamarsi@ekmd.huji.ac.il](mailto:itamarsi@ekmd.huji.ac.il).

This article contains supporting information online at [www.pnas.org/cgi/content/full/0704723105/DC1](http://www.pnas.org/cgi/content/full/0704723105/DC1).

© 2008 by The National Academy of Sciences of the USA

**In Silico Synchronization.** Microarray experiments measure the average RNA level of each gene in a population of cells, and thus are most accurate when using a homogenous population of cells. Partial synchronization causes a severe distortion of microarray results (14). To overcome this problem, we developed a computational approach that takes advantage of the FACS data collected at various time points during the experiment to deconvolve the expression data. The deconvolution algorithm infers gene expression values for the ideal “average single cell”; it does this by using a model learned from the empirically observed distribution of cells and measured expression values recorded at each time point (Fig. 2a). The algorithm is based on the assumption that after release from arrest, each cell proceeds according to its own internal clock. Some of the cells do not emerge from the arrested state, and the remaining cells proceed along the cell cycle at their own rate that, assuming a normal distribution, can be inferred from the FACS data. The inferred “synchronization loss model” can be applied to deconvolve the expression data to generate “single-cell” gene expression profiles. See *Materials and Methods* and [supporting information \(SI\) Methods](#) for complete details. The synchronization loss model

**Fig. 2.** Data deconvolution. (a) Due to loss of synchronization, cells (gray dots) are distributed around the actual time ( $t$ ). Using a synchronization loss model, this distribution can be determined. The actual measurement at time  $t$  is an average of the expression values of the gene (black dot) in all cells and is thus not an accurate representation of the single-cell expression value for this gene at time  $t$ . Using deconvolution on data from multiple time points, we can recover the underlying expression pattern for gene  $i$  ( $u_i$ ). (b) A diagram depicting the percentage of cells entering mitosis at each time point after release from the thymidine block as determined by time-lapse cinematography (gray) and as predicted by the synchronization loss model from the FACS data (black). Note the high correlation between the two distributions ( $R = 0.76$ , ANOVA  $P < 10^{-4}$ ). (c) Expression profile of the BIRC5 gene as measured by microarray analysis of the thymidine block experiment. Raw data (gray triangles) and deconvolved data (black squares).

allows estimation of the percentage of cells at each phase at a given moment. The accuracy of this estimation was confirmed by comparing the time until mitotic entry predicted by our model with direct measurements of mitosis made by using time-lapse cinematography. A very strong agreement is observed between the predicted and observed cell division times (Fig. 2b).

**Identifying Cycling Genes.** RNA was isolated from synchronized foreskin fibroblast cells at 2-h intervals after their release from serum starvation or thymidine block arrest. RNA was also isolated from unsynchronized cultures to generate a reference dataset. RNA expression levels were determined by using Affymetrix microarrays U133A 2.0. As mentioned above, measured expression values from the synchronized cultures were corrected to generate deconvolved expression profiles. The resulting profiles represent single-cell expression values for each gene allowing us to identify cycling genes that cannot be identified when relying on uncorrected measured values. For example, a well known cycling gene, BIRC5, shows only a small fluctuation in its RNA level in the raw data, whereas, after the deconvolution process, the cyclical nature of this gene is obvious (Fig. 2c).

Applying a cyclicity score to the data (*Materials and Methods*) allowed identification of 480 cycling genes. Three lines of evidence support our definition of cycling genes. First, most of the known cycling genes are found among these 480 genes (*SI Appendix*). Second, applying a gene ontology (GO) annotation analysis to the list revealed a high enrichment for cell cycle related categories such as DNA replication, DNA repair, DNA metabolism, mitosis, cell division, and cell cycle regulation (*SI Table 2*). Finally, we confirmed the periodic expression of 10 of the identified cell cycle genes, using RT-PCR (*SI Appendix*).

In addition to genes known to be cycling, the list of 480 cycling genes also includes many genes that were not identified as such in a genome-wide study focused on transformed cells (16), thus vastly expanding the view of cell cycle transcriptional regulation. Assignment of each gene to a cell cycle stage reveals that, as suggested in refs. 4, 7, and 16, the majority of cycling genes are transcribed when they are needed most during the cell cycle (SI Table 3 and SI Appendix).

**Categorizing Cycling Genes.** The study in ref. 16, using the cervical carcinoma cell line HeLa, identified >850 genes that show

periodic expression across the cell cycle. Among these 850 genes, 550 were measured by our platform, and a significant portion of them ( $\approx 40\%$ ,  $P = 0$ ) were identified as cycling in our study as well. To explore the differences between the cell cycles of HeLa and foreskin fibroblast cells as monitored by the two studies, we reanalyzed the Whitfield *et al.* (16) dataset, using the same criteria used in our data analysis. A gene was defined as cycling if it passed a threshold in at least two of the four datasets analyzed (two from each study; see *Materials and Methods*). Using randomization analysis, we determined that the false discovery rate (FDR) using this criterion was  $< 7\%$  (*SI Appendix*). This integrated analysis of both studies resulted in three groups of genes; genes cycling in both primary foreskin fibroblasts and HeLa datasets [“common” (362 genes)], genes cycling only in primary foreskin fibroblasts [“primary FF” (118 genes)], and genes cycling only in the HeLa dataset [“HeLa” (119 genes)] (Fig. 3a).

**Characterizing Cycling Gene Groups.** To distinguish potential differences unique to each of the three gene groups, we analyzed their members for GO annotation and transcription factor binding motifs. As expected, the common set was highly enriched for the major cell cycle categories. Similar enrichment, although to a lesser extent, was found in the primary FF set, whereas there was no enrichment in the HeLa set of genes (Fig. 3b). A similar pattern was observed for binding sites of known cell cycle regulators (17). The common and primary FF sets of genes were enriched for the binding sites of E2F transcription factor (E2F) (22%;  $P < 10^{-12}$  and  $P = 0.01$ , respectively), nuclear factor Y (NFY) (39%;  $P < 10^{-19}$  and  $P = 0.02$ , respectively), and nuclear respiratory factor 1 (NRF1) (36%;  $P < 0.01$  common only). In contrast, the HeLa set of genes were not enriched for motifs of cell cycle regulators. Furthermore, analysis of each group's members, using ChIP on chip data for the transcription factors E2F4, p130, p107 (18), and NFY-B (19), revealed similar findings. Although high percentages of the cycling genes in both common and primary FF datasets are bound by at least one of these factors (27%;  $P < 10^{-63}$  and 24%;  $P < 10^{-15}$ , respectively), only a small portion (5%;  $P = 0.22$ ) of the genes identified in the HeLa set are bound by these factors.

Many cell cycle genes (such as DNA replication genes) are expressed only in proliferating cells, and therefore it is expected that the average expression of cycling genes should be higher in proliferating cells than in arrested cells. To characterize further the cycling gene groups, we used published expression profiles of proliferating and arrested primary fibroblasts (IMR-90) to compare expression levels of the three groups of cycling genes (20). We found that the average expression level of genes in the common and the primary FF groups is significantly higher in primary proliferating cells than in arrested cells ( $P < 10^{-59}$  and  $P < 10^{-18}$ , respectively). In contrast, the average expression level of genes in the HeLa group is not significantly higher in proliferating versus arrested cells ( $P = 0.47$ ; Fig. 4a). Similar results (common,  $P < 10^{-20}$ ; primary FF,  $P < 10^{-7}$ ; and HeLa,  $P = 0.49$ ), were obtained in a reciprocal experiment in which oncogene-induced senescence was bypassed by the transfection of E6/E7 viral proteins (21) (Fig. 4b). The same pattern was also observed in data derived from normal epithelial cells (Fig. 4c and SI Fig. 6). This suggests that the origin of the cells used for the identification of cycling genes (epithelial versus fibroblastic) is not the main cause for the different set of genes identified in each experiment.

Further support for these results was obtained from the analysis of the average expression level of genes, using a panel of 12 normal tissues (22). For each tissue, we compared the average expression level of each set of cycling genes to the average expression level of all genes on the array. We found that the expression levels of cycling genes in the common and primary

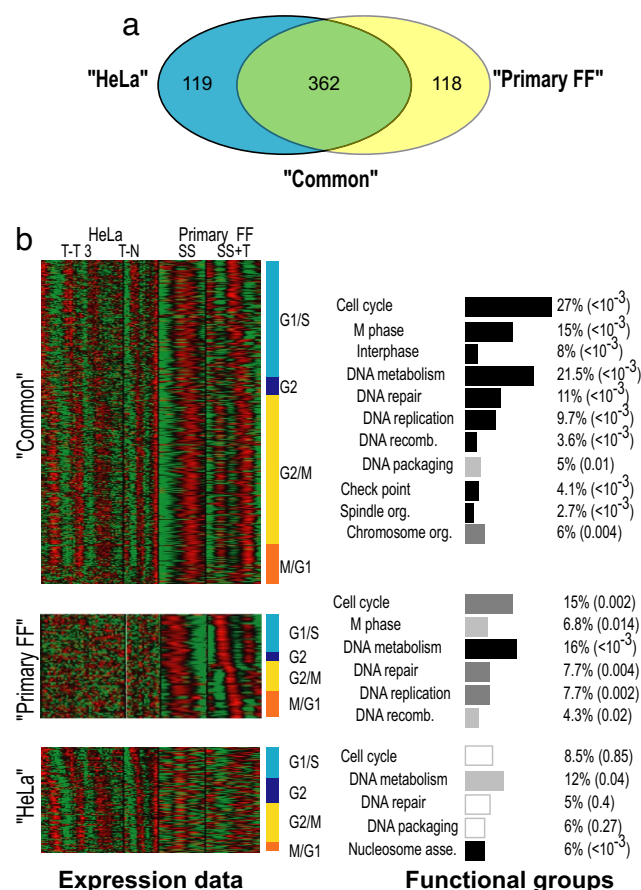
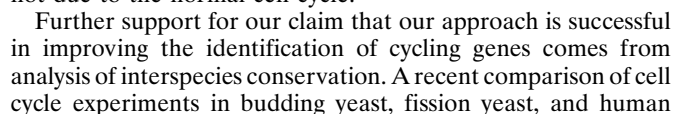


**Fig. 3.** Characterization of three cycling gene groups. (a) Venn diagram depicting the overlap between cycling genes identified in Whitfield's (16) and our datasets. The numbers in each section of the diagram reflect the number of genes in each group (see [SI Table 5](#) for a list of all of the cycling genes). (b) Expression data for each group of cycling genes (log ratio to unsynchronized culture) is represented by color, using a heat map, where red indicates induced expression and green indicates repressed expression. For the HeLa cells, we used data published in ref. 16 of the Thy-Thy 3 (T-T3) and Thy-Noc (T-N) experiments. For the primary FF cells, we used the deconvolved expression data for the serum starvation (SS) and thymidine block (T) experiments. The genes within a group have been ordered (vertically) according to their assigned cell cycle stage, which is indicated on the right of the heat maps. Enrichment analysis of each group's members for functional cell cycle GO categories is represented by rectangles next to that group (for the full analysis, see [SI Table 2](#)). The length of a rectangle depicts the percentage of cycling genes that fall into the category (2.7–27%), and the color depicts the significance of the enrichment. The significance levels (in parentheses) were corrected for multiple hypotheses (see *Materials and Methods*) and are indicated by three levels of gray color for  $P < 0.05$ ,  $< 0.005$  and  $< 0.001$ . White rectangles indicate no enrichment ( $P > 0.05$ ).

FF groups are significantly low in most tissues and are expressed at considerably higher levels only in the thymus and bone marrow samples, which are the only two tissues in our analysis that contain a high percentage of proliferating cells. In sharp contrast, the genes of the HeLa group do not exhibit this distinctive pattern of tissue expression (Fig. 4d). These results are consistent with the conclusion that our method accurately identifies cycling genes in primary cells.

**The Primary FF Group Contains Cycling Genes Unique to Normal Cells.** It is possible that some of the genes identified as cycling in our dataset were not identified as such in the Whitfield study (16), owing to differences in experimental procedures. However, we propose that some of these genes are cycling only in normal cells







learned for our model were further validated by using time-lapse cinematography. See [SI Methods](#) for details.

**Correcting for Partial Reentry.** After normalization, expression data were corrected for the percentage of cells reentering cell cycle. This percentage was determined in our model, using FACS as discussed above. Let  $Y_0$  be the measured expression of a gene in time point 0 (before release,  $G_0$ ) and  $Y_t$  be the measured expression in time point  $t$ . If the fraction of cells entering the cell cycle is  $P$ , then the measured value at time  $t$  is from a mixture of cells,  $P$  of which are cycling and the rest are not. This can be formally stated as follows:  $Y_t = PC_t + (1 - P)Y_0$ .

From this equation, we can derive the expression value for the cycling cells,  $C_t$ , which is used in subsequent analysis. We next computed log ratios, using duplicate measurements of unsynchronized populations.

**Deconvolving Expression Data.** Using the learned synchronization loss model, the corrected expression data were deconvolved. The goal of a deconvolution algorithm is to obtain the actual expression value for each time point from measurements of cells that are distributed around that time point. The deconvolution method uses continuous representation to determine the underlying expression values. See Fig. 2a and [SI Appendix](#) for more details and a discussion of relative peak heights.

**Scoring Deconvolved Expression Profiles.** The resulting expression profiles were scored by using Fourier transform (4). To determine a score cutoff, we randomly permuted both datasets and repeated the above steps for each of these (random) datasets. Similarly, we have randomized two datasets from ref. 16 (the T-T3 and the T-N datasets) that showed high levels of synchronization (40). Using scores from the randomized datasets, we have determined a cutoff score. A gene was included in the resulting cycling lists (common, primary FF, and HeLa) if it passed this score for at least two of the datasets. Note that the primary FF group also contains 35 genes that were not measured in the Whitfield experiment (16). Based on the randomization analysis, the false discovery rate was 1% for genes identified as primary FF or HeLa and 6% for genes identified as common. See [SI Appendix](#) for a detailed discussion addressing (i) potential synchronization artifacts, (ii) the specificity and sen-

sitivity of the deconvolution method, and (iii) the improvement in data analysis achieved by the deconvolution step.

**Phase Assignment.** Genes were assigned to phases by computing their correlation with previously annotated cell cycle genes, as described in ref. 16. Six genes from a list of known cell cycle genes (16) were used ([SI Table 4](#)). We computed the correlation of each of the predicted cycling genes and the averages of the known phase genes and assigned the gene to the phase with the highest correlation. This process was repeated for both datasets. For 56% of the genes, the two datasets agreed on the phase assignment. For the majority of the rest, they were assigned to two consecutive phases (such as to G<sub>2</sub>/M in one and M/G<sub>1</sub> in the second). In such cases, we used the assignment from the dataset in which this gene scored higher.

**Expression Data Analysis.** Data were downloaded from Gene Expression Omnibus database (accession nos. GSE2487, GSE4888, GDS426, GDS1209, and GDS181) or obtained from the researchers (20). Each experiment was normalized by the average expression in the experiment. Multiple experiments of the same type were combined. Significant differences between groups were assessed by  $t$  test. The tumor proliferation clusters of breast (23) and lymphomas (24) were combined and the overlap with the common and primary FF groups was determined. The rank statistics is described in the [SI Appendix](#).

**Statistical Analysis of GO and Motif Enrichment.** GO annotation enrichment was calculated by using the STEM program (41), and the reported hypergeometric  $P$  values were corrected for multiple hypothesis, using randomization. Motifs enrichment was determined by the PRIMA software (17).

**ACKNOWLEDGMENTS.** We thank Shlomit Farkash-Amar for statistical analysis. This work was supported by grants from the Association for International Cancer Research, European Commission Sixth Framework Programme Contract 503576, and the Binational Science Foundation (to I.S.); U.S. National Science Foundation Career Award 0448453 and the Tobacco Settlement Grant from the Pennsylvania Department of Health (to Z.B.-J.); National Institutes of Health Grant CA077245-11 (to B.D.D.); and the German Federal Ministry of Research and Education through the National Genome Research Network Grant 01 GR 0450 (to B.B. and R.E.).

- Whitfield ML, George LK, Grant GD, Perou CM (2006) *Nat Rev Cancer* 6:99–106.
- Cooper S, Shedden K (2003) *Cell Chromosome* 2:1.
- Cho RJ, Campbell MJ, Winzler EA, Steinmetz L, Conway A, Wodicka L, Wolfsberg TG, Gabriellian AE, Landsman D, Lockhart DJ, et al. (1998) *Mol Cell* 2:65–73.
- Spellman PT, Sherlock G, Zhang MQ, Iyer VR, Anders K, Eisen MB, Brown PO, Botstein D, Futcher B (1998) *Mol Biol Cell* 9:3273–3297.
- Oliva A, Rosebrock A, Ferrezuelo F, Pyne S, Chen H, Skiena S, Futcher B, Leatherwood J (2005) *PLoS Biol* 3:e225.
- Peng X, Karuturi RK, Miller LD, Lin K, Jia Y, Kondu P, Wang L, Wong LS, Liu ET, Balasubramanian MK, et al. (2005) *Mol Biol Cell* 16:1026–1042.
- Rustici G, Mata J, Kivinen K, Lio P, Penkett CJ, Burns G, Hayles J, Brazma A, Nurse P, Bahler J (2004) *Nat Genet* 36:809–817.
- Bar-Joseph Z, Farkash S, Gifford DK, Simon I, Rosenfeld R (2004) *Bioinformatics* 20(Suppl 1):i23–i30.
- Lu X, Zhang W, Qin ZS, Kwast KE, Liu JS (2004) *Nucleic Acids Res* 32:447–455.
- Qiu P, Jane Wang Z, Ray Liu KJ (2005) *Conf Proc IEEE Eng Med Biol Soc* 5:4826–4829.
- Iyer VR, Eisen MB, Ross DT, Schuler G, Moore T, Lee JC, Trent JM, Staudt LM, Hudson J, Jr, Boguski MS, et al. (1999) *Science* 283:83–87.
- Tobey RA, Valdez JG, Crissman HA (1988) *Exp Cell Res* 179:400–416.
- Cho RJ, Huang M, Campbell MJ, Dong H, Steinmetz L, Sapinoso L, Hampton G, Elledge SJ, Davis RW, Lockhart DJ (2001) *Nat Genet* 27:48–54.
- Shedden K, Cooper S (2002) *Proc Natl Acad Sci USA* 99:4379–4384.
- Simon I, Siegfried Z, Ernst J, Bar-Joseph Z (2005) *Nat Biotechnol* 23:1503–1508.
- Whitfield ML, Sherlock G, Saldanha AJ, Murray JJ, Ball CA, Alexander KE, Matese JC, Perou CM, Hurt MM, Brown PO, et al. (2002) *Mol Biol Cell* 13:1977–2000.
- Elkon R, Linhart C, Sharan R, Shamir R, Shilo Y (2003) *Genome Res* 13:773–780.
- Cam H, Balciunaite E, Blais A, Spektor A, Scarpulla RC, Young R, Kluger Y, Dynlacht BD (2004) *Mol Cell* 16:399–411.
- Ceribelli M, Alcalay M, Vigano MA, Mantovani R (2006) *Cell Cycle* 5:1102–1110.
- Narita M, Narita M, Krizhanovsky V, Nunez S, Chicas A, Hearn SA, Myers MP, Lowe SW (2006) *Cell* 126:503–514.
- Collado M, Gil J, Efeyan A, Guerra C, Schuhmacher AJ, Barradas M, Benguria A, Zaballos A, Flores JM, Barbacid M, et al. (2005) *Nature* 436:642.
- Yanai I, Benjamin H, Shmushov M, Chalifa-Caspi V, Shklar M, Ophir R, Bar-Even A, Horn-Saban S, Safran M, Domany E, et al. (2005) *Bioinformatics* 21:650–659.
- Perou CM, Sorlie T, Eisen MB, van de Rijn M, Jeffrey SS, Rees CA, Pollack JR, Ross DT, Johnsen H, Akslen LA, et al. (2000) *Nature* 406:747–752.
- Alizadeh AA, Staudt LM (2000) *Curr Opin Immunol* 12:219–225.
- Tabach Y, Milyavsky M, Shats I, Brosh R, Zuk O, Yitzhaky A, Mantovani R, Domany E, Rotter V, Pilpel Y (2005) *Mol Syst Biol* 1:2005 0022.
- Detwiller KY, Fernando NT, Segal NH, Ryeom SW, D'Amore PA, Yoon SS (2005) *Cancer Res* 65:5881–5889.
- Su AI, Wiltshire T, Batalov S, Lapp H, Ching KA, Block D, Zhang J, Soden R, Hayakawa M, Kreiman G, et al. (2004) *Proc Natl Acad Sci USA* 101:6062–6067.
- Lu Y, Mahony S, Benos PV, Rosenfeld R, Simon I, Breeden LL, Bar-Joseph Z (2007) *Genome Biol* 8:R146.
- Lyakhovich A, Surrallés J (2006) *Cancer Lett* 232:99–106.
- Takayama T, Mogi Y, Kogawa K, Yoshizaki N, Muramatsu H, Koike K, Semba K, Yamamoto T, Niitsu Y (1993) *Int J Cancer* 54:875–879.
- Rouault JP, Rimokh R, Tessa C, Paranhos G, French M, Duret L, Garocchio M, Germain D, Samarut J, Magaud JP (1992) *EMBO J* 11:1663–1670.
- Liu Y, Corcoran M, Rasool O, Ivanova G, Ibbotson R, Grandt D, Iyengar A, Baranova A, Kashuba V, Merup M, et al. (1997) *Oncogene* 15:2463–2473.
- Sironi E, Cerri A, Tomasini D, Sirchia SM, Porta G, Rossella F, Grati FR, Simoni G (2004) *J Cutan Pathol* 31:318–322.
- Borrow J, Shearman AM, Stanton VP, Jr, Becher R, Collins T, Williams AJ, Dube I, Katz F, Kwong YL, Morris C, et al. (1996) *Nat Genet* 12:159–167.
- Golub TR, Slonim DK, Tamayo P, Huard C, Gaasenbeek M, Mesirov JP, Coller H, Loh ML, Downing JR, Caligiuri MA, et al. (1999) *Science* 286:531–537.
- Fu L, Pelicano H, Liu J, Huang P, Lee C (2002) *Cell* 111:41–50.
- Keats JJ, Maxwell CA, Taylor BJ, Hendzel MJ, Chesi M, Bergsagel PL, Laratt LM, Mant MJ, Reiman T, Belch AR, et al. (2005) *Blood* 105:4060–4069.
- Ewen ME, Xing YG, Lawrence JB, Livingston DM (1991) *Cell* 66:1155–1164.
- Lozano JJ, Kalko SG (2006) *Appl Bioinformatics* 5:45–47.
- Wichert S, Fokianos K, Strimmer K (2004) *Bioinformatics* 20:5–20.
- Ernst J, Bar-Joseph Z (2006) *BMC Bioinformatics* 7:191.
- Talbi S, Hamilton AE, Vo KC, Tulac S, Overgaard MT, Dosiou C, Le Shay N, Nezhad CN, Kempson R, Lessey BA, et al. (2006) *Endocrinology* 147:1097–1121.